THE JOURNAL OF PHYSICAL CHEMISTRY B

Article

pubs.acs.org/JPCB

Changes in the Microenvironment of Nitroxide Radicals around the Glass Transition Temperature

Enrica Bordignon,*[,†,‡] Anna I. Nalepa,[§] Anton Savitsky,[§] Lukas Braun,[†] and Gunnar Jeschke[†]

[†]Laboratory of Physical Chemistry, ETH Zurich, Vladimir-Prelog-Weg 2, 8093 Zurich, Switzerland

[‡]Berlin Joint EPR Laboratories, Department of Experimental Physics, Free University of Berlin, Arnimallee 14, 14195 Berlin, Germany

[§]Max Planck Institute for Chemical Energy Conversion, Stiftstrasse 34−36, 45470 Mülheim an der Ruhr, Germany

Supporting Information

ABSTRACT: For structural characterization by pulsed EPR methods, spin-labeled macromolecules are routinely studied at cryogenic temperatures. The equilibration of the conformational ensemble during shock-freezing occurs to a good approximation at the glass transition temperature (T_g). In this work, we used X-band power saturation continuous wave (cw) EPR to obtain information on the glass transition temperatures in the microenvironment of nitroxide radicals in solvents or bound to different sites in proteins. The temperature dependence of the saturation curve of nitroxide probes in pure glycerol or *ortho*-terphenyl showed detectable transitions at the respective T_g values, with the latter solvent characterized by a sharper change of the saturation properties, according to its higher fragility. In contrast, nitroxide probes in a glycerol/water mixture showed a discontinuity in the saturation properties close to the expected glass transition temperature, which made the determination of T_g complicated. Low-temperature W-band cw EPR and W-band ELDOR-detected NMR experiments demonstrated that the discontinuity is due to local rearrangements of H-bonds between water molecules and the nitroxide reporter group. The change in the network of H-bonds formed between the nitroxide and water molecules that occurs around T_g was found to be site-dependent in spin-labeled proteins. This effect can therefore be modulated by neighboring residues with different steric hindrances and/or charge distributions and possibly by the glycerol enrichment on protein surfaces. In conclusion, if the thermal history of the sample is carefully reproduced, the nitroxide probe is extremely sensitive in reporting site-specific changes in the H-bonding to water molecules close to T_g and local glass transition temperatures in spin-labeled macromolecules.

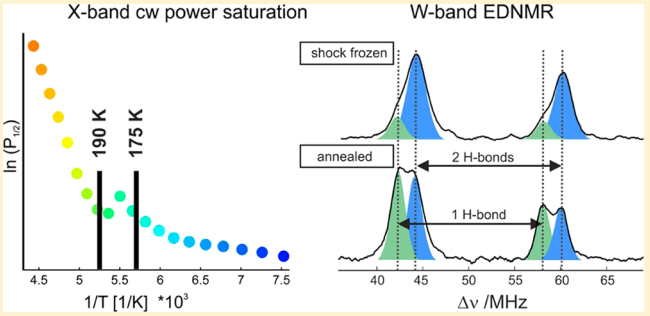

INTRODUCTION

Various EPR techniques can be applied to characterize the microenvironment of nitroxide spin labels at both room and cryogenic temperatures. The g and hyperfine tensor values (in particular g_{xx} and A_{zz}) of nitroxide radicals provide information about the polarity (electric fields along the NO bond) and proticity (H-bonds toward the NO group) of their microenvironment,[1] which can be translated into topological properties relevant for protein science. An example is the mapping of the proton channel of bacteriorhodopsin by low-temperature W-band cw EPR.[2] In addition, a characteristic heterogeneity was discovered in the g_{xx} region of W-band cw EPR spectra, due to the existence of three distinct populations of nitroxides in water-containing frozen solutions, with zero, one, or two H-bonds toward the nitroxide group. These populations vary in their relative ratios depending on the availability of H-bond donor groups, mostly water molecules, in the vicinity of the spin label.[3] The existence of these three distinct components, characterized by three respective g_{xx} parameters, was also recently addressed with better spectral resolution at higher magnetic fields,[4] and it was proven to constitute the fingerprint of the microenvironment of the nitroxide radical in frozen solutions. The use of ELDOR-detected NMR (EDNMR) added another sensitive tool to disentangle the variations in the A_{zz} parameter that correlate with the nitroxide populations with distinct H-bonds.[4,5] In terms of water accessibility toward nitroxides, ESEEM techniques at cryogenic temperatures are also used to explore the concentration of ^{2}H around spin-labeled sites (in samples containing deuterated water and/or glycerol) (see, for example, refs 6 and 7). To overcome the problem of freezing the samples to address water accessibility toward nitroxides, power saturation cw EPR methods are used, which allow obtaining the accessibility of nitroxides toward paramagnetic reagents, soluble either in aqueous or lipid environments.[8−11] Other methods that provide information on protein topology at the water−membrane

Special Issue: Wolfgang Lubitz Festschrift

Received: April 29, 2015
Revised: August 12, 2015
Published: August 12, 2015

DOI: 10.1021/acs.jpcb.5b04104
J. Phys. Chem. B 2015, 119, 13797−13806

interfaces include saturation recovery techniques[12] and Overhauser DNP.[13,14]

Most pulsed EPR experiments are performed at cryogenic temperatures, and it was earlier recognized that at around 170−180 K a solvent phase transition occurs in water/glycerol mixtures.[15] The cooling rates also play a certain role in determining the conformation of the protein and the ensemble of trapped spin label rotamers, hence the interspin distance distribution between two spin-labeled sites, as was demonstrated on T4-lysozyme.[16] In the case of nitroxide spin labels, the molecular ensemble of rotamers trapped at cryogenic temperature is thought to be correlated to the conformational equilibrium at the glass transition temperature. The most commonly used matrix for protein studies consists of water and glycerol (10−50% v/v); therefore, a temperature of 175 K was originally chosen as representative of the glass transition temperature for calculation of the (1-oxyl-2,2,5,5-tetramethyl-Δ3-pyrroline-3-methyl) methanethiosulfonate spin label (MTSL) rotamers in the software MMM.[17] Later it was found that rotamer simulations at 298 K show better agreement with experiments,[18,19] most likely due to error compensation. Systematic further development of predictions of conformation ensembles of the spin label side group requires better understanding of its conformational equilibria near the glass transition temperature. In fact, when a solution is cooled and turns into a glassy state, several properties such as heat capacity, density, as well as the probability of the H-bond formation will show a pronounced change at the glass transition temperature. It has already been demonstrated by Miwa et al.[20−22] that power saturation cw EPR performed on spin-labeled polymers is effective in determining local glass transition temperatures, which were found to be in agreement with those obtained by classic differential scanning calorimetry (DSC) methods.

Here, we apply X-band power saturation cw EPR to extract local glass transition temperatures in the nitroxide microenvironment in the presence and absence of water. We complement this analysis with relaxation measurements via pulsed EPR as well as with W-band cw EPR and EDNMR measurements, to monitor closely the microenvironment of the nitroxide in terms of H-bond network.

We used binary mixtures (nitroxide/glycerol; nitroxide/*ortho*-terphenyl), ternary mixtures (nitroxide/water/glycerol), as well as two site-directed spin-labeled proteins in aqueous buffers containing glycerol as a cryoprotectant. We found that, in binary systems with pure glycerol or pure *ortho*-terphenyl, the temperature dependence of the saturation obtained via power saturation cw EPR provides an indication of the local glass transition temperature around nitroxide probes, similar to what was found for spin-labeled polymers.[20−22] However, in water−glycerol mixtures, the analysis of the power saturation curves as well as the trend of relaxation rates vs temperature is more complicated and the curves present a discontinuity close to the glass transition temperature of the bulk solvent. We found that the thermal history of the sample (e.g., annealing above 180 K) modifies the properties of the microenvironment of the nitroxide reporter group and therefore influences the appearance of the discontinuity. The origin of the hysteresis was found to be the rearrangement of the water H-bond network toward the nitroxide close to the glass transition temperature.

MATERIALS AND METHODS

Sample Preparation for Power Saturation cw EPR and T_1 and T_m Determination. A 0.5 mM solution of 3-carbamoyl-2,2,5,5-tetramethyl-3-pyrrolin-1-oxyl (abbreviated as SL1) was prepared in a glycerol-D_8/buffer mixture (50% or 30% v/v, the buffer used was 50 mM MOPS, 25 mM NaCl, pH 6.8) and in pure glycerol-D_8 (the latter was prepared using the nitroxide powder directly mixed with glycerol-D_8). A 0.5 mM solution of SL1 in *ortho*-terphenyl-D_{14} (DOTP) was also prepared using the powder components; mixing was ensured by warming the mixture with a heat gun above the melting point of OTP (332 K) and freezing it in liquid nitrogen. Subsequently, an aliquot of the mixture was inserted into the quartz tube for the measurements.

Two spin-labeled protein samples were investigated by power saturation cw EPR. The T4-lysozyme C96 mutant was spin-labeled with MTSL (Toronto Research Canada). The protein variant was purified as previously described[23,24] starting from a plasmid obtained from Addgene (Cambridge, MA). The spin-labeled protein was concentrated to ca. 150 μM, in 50 mM MOPS, 25 mM NaCl, pH 6.8; 50% v/v glycerol-D_8 was added prior to shock freezing of the sample in the EPR tube. The maltose binding protein MalE carrying a cysteine at position 36 was purified and spin-labeled as previously described.[25] The spin-labeled protein was concentrated to ca. 200 μM, in 50 mM Tris/HCl, pH 7.5; 50% v/v glycerol-D_8 was added prior to shock freezing of the sample in the EPR tube.

Power Saturation cw EPR. The samples were loaded into a 1.8 mm outer diameter (o.d.) quartz tube, which was inserted inside a 3 mm o.d. quartz tube. All samples had the same thermal history: after equilibration at RT (363 K for DOTP), samples were shock-frozen in liquid nitrogen and inserted in the precooled cavity at 135 K. The cw EPR spectra were recorded stepwise each 5 K from 135 to 230 K (glycerol-D_8) or 270 K (DOTP), allowing the sample to equilibrate to the new temperature for 25 min. The temperature of the sample was additionally calibrated using a thermocouple inserted in a 3 mm o.d. tube containing a water/glycerol solution. All power saturation cw EPR measurements were performed at the X-band in an Elexsys E500 spectrometer equipped with a super high-Q cavity (Bruker) and a N_2 flow cryostat. Spectra were detected at 0.2 mT modulation amplitude, 10 or 100 kHz modulation frequency, 2.56 ms time constant, and 10 ms conversion time with a sweep time of 5 s for each microwave power. The detection of the power saturation curves at one temperature under these conditions took 200 s.

In the low temperature regime, rapid passage effects can perturb the cw detection at both 10 and 100 kHz.[26,27] Therefore, we tested both modulation frequencies and compared the resulting $\ln(P_{1/2})$ vs $1/T$ and found no appreciable differences in the characteristic temperature trend. The power saturation curve can be plotted either with the value of the double integral of the EPR derivative spectrum (V_R in eq 1) or with the peak-to-peak intensity of the central EPR derivative line (V_R in eqs 2 and 3) for homogeneous (eq 2) or inhomogeneous (eq 3) cases. Note that eq 3 is also valid for the value of the double integral for inhomogeneous cases. The proportionality to the saturation factor $S = \gamma^2 H_1^2 T_1 T_2$ is described in eqs 1−3, with γ being the gyromagnetic ratio of the spin probe, H_1 the microwave magnetic field strength, and T_1 and T_2 the longitudinal and transverse relaxation times, respectively.

double integral (hom. case):

$$V_R \propto \frac{\sqrt{S}}{(1 + S)^{1/2}} \quad (1)$$

DOI: 10.1021/acs.jpcb.5b04104
J. Phys. Chem. B 2015, 119, 13797−13806

Peak-to-peak intensity (deriv. spectrum) (hom. case):

$$V_R \propto \frac{\sqrt{S}}{(1+S)^{3/2}} \tag{2}$$

Peak-to-peak intensity or double integral (inhom. case):

$$V_R \propto \frac{\sqrt{S}}{(1+S)^{1/2}} \tag{3}$$

The peak-to-peak intensity of the central EPR line (I_{pp}) was plotted vs the square root of the microwave power (P). The fit was performed according to

$$I_{pp} = a\frac{\sqrt{P}}{\left(1+(2^{1/\varepsilon}-1)\frac{P}{P_{1/2}}\right)^{\varepsilon}} \tag{4}$$

with

$$P_{1/2} = \frac{(2^{1/\varepsilon}-1)}{\gamma^2 T_1 T_2} \qquad S = \frac{H_1^2(2^{1/\varepsilon}-1)}{P_{1/2}} \tag{5}$$

The parameter ε was restricted in the fitting to the range $^1/_2$:$^3/_2$ to account for the homogeneous and inhomogeneous line broadening, while a was a free scaling factor.

It is worth noting that some analyses of the T_g of polymers by power saturation cw EPR experiments[20−22] calculated the double integral of the EPR spectra (eq 1) erroneously assuming a proportionality as in eq 6, which is valid only for the maximum intensity of the absorption signal at $\Delta\omega_0 = 0$:

maximum absorption (hom. case):

$$V_R \propto \frac{\sqrt{S}}{1+S} \tag{6}$$

T_1 and T_m Measurements. Relaxation measurements were performed at X band in the Bruker Elexsys E580 spectrometer equipped with a split ring (MS3, Bruker) resonator and a helium flow cryostat. The samples were inserted in 3.0 mm o.d. quartz tubes. Experiments were performed in quenched and annealed conditions. In quenched conditions, all samples had the same thermal history: the tube equilibrated at RT (363 K for DOTP) was shock-frozen in liquid nitrogen and inserted in the precooled cavity at 140 K. The measurements were performed stepwise each 5 K from 140 to 210 K (glycerol-D_8) or 270 K (DOTP), allowing the sample to equilibrate to the new temperature for 12 min. The temperature of the sample was calibrated using a thermocouple inserted in a 3 mm o.d. tube containing a solution of water/glycerol. The buffer/glycerol-D_8/SL1 system was additionally measured under annealed conditions: the full set of measurements was repeated on the sample shock-frozen in liquid nitrogen and annealed for >24 h in the −80 °C freezer (generally used for cryo-storage of samples as an alternative to liquid nitrogen). The two-pulse ESEEM (2P-ESEEM) traces were recorded with a $\pi/2$-τ_1-π pulse sequence with $\pi/2$ = 16 ns pulse length and a starting interpulse delay of τ_1 = 200 ns that was incremented in steps of 8 ns. The T_m values were extracted from a monoexponential fit of the 2P-ESEEM traces, without considering the deuterium modulations. The inversion recovery traces were recorded with a $\pi/2$-τ-π detection sequence using $\pi/2$ = 52 ns pulse length, that was preceded by a nonselective 32 ns π-pulse. The first interpulse delay was set to τ = 500 ns, and incremented by 1000 ns. The T_1 values were extracted as the time point at which the normalized inversion recovery trace decays to 1/e of its initial value. The logarithm of the relaxation rates $1/T_1$ was then plotted as a function of inverse temperature, $1/T$.

Sample Preparation for W-Band cw EPR and EDNMR. The perdeuterated nitroxide spin probe 3-hydroxymethyl-2,2,5,5-tetramethylpyrrolin-1-oxyl (termed as SL2) used in this study was synthesized as described previously.[28] The solvents D_2O and glycerol-D_8 were obtained from Deutero GmbH and Sigma-Aldrich, respectively. SL2 was directly dissolved in D_2O, and subsequently, the nitroxide stock solution was mixed with glycerol-D_8 to obtain the predefined cryoprotectant concentration (% v/v) with about 1 mM final nitroxide concentration. For T4-lysozyme spin-labeled with MTSL at position C96, a final concentration of 400 μM in aqueous buffer containing 50% glycerol-D_8 was used. The samples were transferred into quartz capillaries (i.d. 0.6 mm) for the W-band EPR measurements. A glass-type frozen solution was obtained by transferring the sample, either equilibrated at RT or shock-frozen in liquid nitrogen, into the precooled EPR cryostat at about 85 K. Both types of freezing procedures yielded the same results. For all samples, W-band cw EPR and EDNMR spectra were recorded with the same thermal history: the sample equilibrated at RT was inserted into the EPR cavity precooled at 80−90 K and cw EPR and EDNMR spectra were recorded at 80 K. Subsequently, the sample was annealed at 200 K (for SL2 in D_2O/glycerol-D_8 mixtures or spin-labeled T4 lysozyme) or at 230 K (for SL2 dissolved in pure glycerol-D_8) for 1 h. After cooling down of the sample to 80 K, cw EPR and EDNMR spectra were recorded again at 80 K with the same experimental settings as before annealing. The temperature of the sample was additionally controlled using an external thermocouple. The reproducibility of the results was ensured by performing some of the experiments twice.

W-Band EPR and EDNMR. The W-band cw EPR and EDNMR experiments were performed on a modified Bruker Elexsys E680 spectrometer operating at about 94 GHz.[5] For cw EPR experiments, the magnetic field was modulated at 100 kHz with an amplitude of 0.1 mT. The EDNMR experiments made use of two-pulse Hahn-echo detection at microwave frequency ν_1, matched to the cavity resonance. The high-turning angle (HTA) microwave pulse was applied at the microwave frequency ν_2. The spectra were acquired by continuously sweeping ν_2 at a fixed magnetic field, in steps of 70 kHz. The length and amplitude of the HTA pulse were adjusted to obtain an ELDOR π-pulse on the forbidden transition of interest at the g_{zz}, $m_I = -1$ field position. The HTA pulse length was set to 2.5 μs at a pulse amplitude of 6.4×10^7 rad/s (for SL2) or 1.8 μs at 4.5×10^7 rad/s (for spin-labeled T4-lysozyme). The detection sequence was set 7.5 μs after the HTA pulse to ensure the decay of electron-spin coherence. The length of the detection $\pi/2$-pulse was set to 100 ns, and the pulse separation to 1 μs. The echo was integrated over 1.4 μs (for SL2) or 1.2 μs (for spin-labeled T4-lysozyme) around its maximum for optimal resolution. For the two-dimensional EDNMR data surface, EDNMR traces were recorded in the field range of 1.2 mT around the g_{zz}, $m_I = -1$ spectral field position. A repetition rate of 330 Hz was used to allow the echo signal to restore between consecutive pulse trains. The EDNMR data were analyzed according to the previously reported procedure.[5]

RESULTS

First we performed control experiments using power saturation cw EPR (see Materials and Methods) with the nitroxide spin probe SL1 dissolved in pure perdeuterated glycerol (glycerol-D_8) or in perdeuterated *ortho*-terphenyl (DOTP). These simple

DOI: 10.1021/acs.jpcb.5b04104
J. Phys. Chem. B 2015, 119, 13797−13806

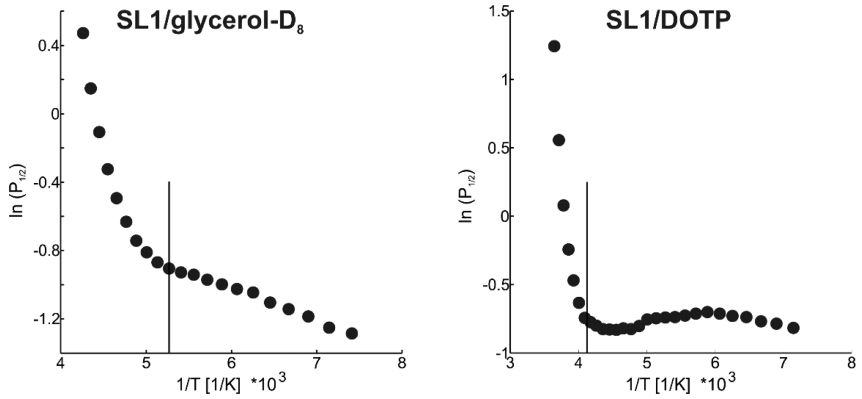

Figure 1. Plot of $\ln(P_{1/2})$ vs $1/T$ for SL1 in pure glycerol-D_8 (left panel) and in DOTP (right panel). The vertical lines represent the 190 and 243 K glass transition temperatures of the respective solvents. Examples of cw EPR spectra and power saturation curves of SL1 in glycerol-D_8 at 140 and 200 K are shown in Figure S1. The effect of different modulation frequencies (10 or 100 kHz) in the $\ln(P_{1/2})$ vs $1/T$ curves for SL1 in glycerol-D_8 is shown in the left panel of Figure S2.

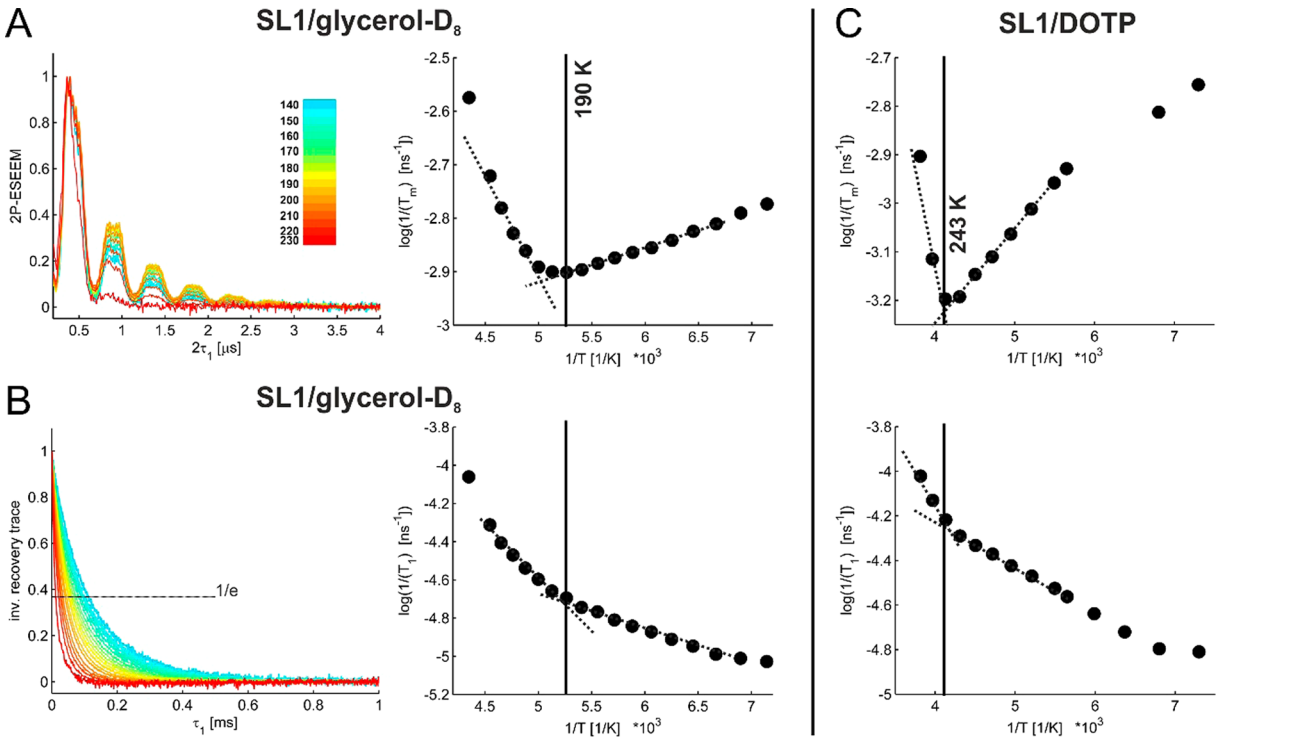

Figure 2. Temperature dependence of the relaxation rates. (A) Left: 2P-ESEEM traces recorded for SL1 in pure deuterated glycerol at different temperatures from 140 K (cyan) to 230 K (red) (see color legend). Right: Plot of $\log(1/T_m)$, with T_m expressed in ns, vs $1/T$. The trend of T_m values was extracted using a monoexponential fit of the 2P-ESEEM traces, without explicitly taking into account the deuterium modulations. The vertical line marks the T_g of pure glycerol (190 K). The dotted lines guide the eye to highlight the visible change in slope at T_g. (B) Left: Inversion recovery traces after baseline subtraction, normalization, and multiplication by −1 recorded on SL1 in pure deuterated glycerol at different temperatures from 140 K (cyan) to 230 K (red) (same color legend as in panel A). Right: Plot of $\log(1/T_1)$, with T_1 expressed in ns, vs $1/T$. (C) SL1 in pure DOTP. Upper panel, plot of $\log(1/T_m)$, with T_m expressed in ns, vs $1/T$; bottom panel, plot of $\log(1/T_1)$ vs $1/T$. The temperature range is from 137 to 272 K (see Figure S3C for the primary data). The vertical lines represent the 243 K glass transition temperature of *ortho*-terphenyl. The dotted lines guide the eye to highlight the distinct change in slope at T_g.

binary systems with very distinct glass transition temperatures (190 K for pure glycerol[29] and 243 K for pure *ortho*-terphenyl[30,31]) are ideal to verify the applicability of this technique to spin probes dissolved in solvents. The power saturation curves were fitted using eq 4, and the value of the microwave power at which the peak-to-peak intensity reaches half of its putative intensity in the absence of saturation ($P_{1/2}$) was extracted (see Figure S1 and the Materials and Methods section). Figure 1 shows the $\ln(P_{1/2})$ values plotted vs the inverse of the temperature for both samples. A smooth change in the saturation properties of the nitroxide reporter group can be detected in glycerol around the solvent glass transition temperature (190 K, see vertical line in the left panel of Figure 1). In contrast, a sharper transition is detected in DOTP around 243 K (see vertical line in the right panel of Figure 1).

To corroborate the temperature dependence of $\ln(P_{1/2})$ presented in Figure 1, we additionally analyzed the temperature dependence of the phase memory time T_m via 2P-ESEEM and of

DOI: 10.1021/acs.jpcb.5b04104
J. Phys. Chem. B 2015, 119, 13797−13806

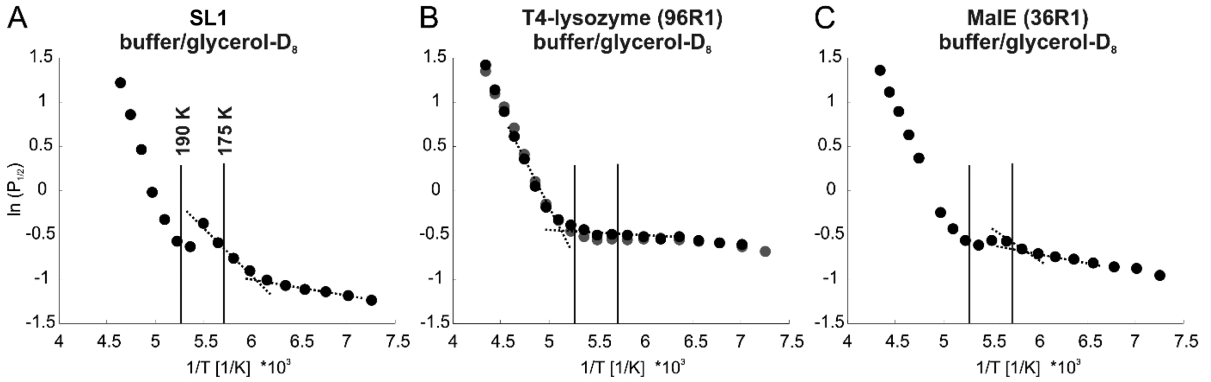

Figure 3. Temperature dependence of the EPR saturation of three different nitroxide probes in water-containing environments. (A) Plot of $\ln(P_{1/2})$ vs $1/T$ for SL1 in aqueous buffer with 50% v/v glycerol-D_8. The vertical lines represent the 175 K (T_g used in MMM for water/glycerol mixture) and 190 K (T_g for pure glycerol). A first change in slope appears at $T < 175$ K, and a discontinuity is evident in between the two vertical lines. The dotted lines guide the eye to highlight the first visible change in slope. (B) Plot of $\ln(P_{1/2})$ vs $1/T$ for the MTSL spin label covalently bound to the engineered cysteine at position 96 (named 96 R1) in T4-lysozyme in aqueous buffer containing 50% (black dots) or 30% (gray dots) v/v glycerol-D_8. The vertical lines represent the 175 and 190 K. A first change in slope appears at around 190 K, and no discontinuity is detected in between the two vertical lines. (C) Plot of $\ln(P_{1/2})$ vs $1/T$ for the MTSL spin label covalently attached to the maltose binding protein MalE (named 36 R1) in aqueous buffer with 50% v/v glycerol-D_8. The vertical lines represent the 175 and 190 K. A first change in slope appears close to 175 K, and a small but detectable discontinuity is present in between the two vertical lines.

the longitudinal relaxation time T_1 via inversion recovery for both samples (see Figure 2 and the Materials and Methods section). Due to strong deuterium modulation, the fit of the 2P-ESEEM traces can provide only a trend for the temperature dependence of the T_m values, which were obtained by a simple monoexponential fit of the 2P-ESEEM time traces. We refrained from stretched exponential fits that may, in principle, appear more appropriate in the context of a study of the glass transition, as such fits would be less stable and interpretation of the stretched exponent would be complicated due to the presence of several contributions to relaxation, with some of them causing nonexponential relaxation even in a crystalline environment. Notably, to prolong the transverse relaxation time of spin-labeled proteins, deuteration of the solvent is routinely performed; therefore, deuterium modulation will always affect the T_m analysis in protein samples. The T_1 values were extracted as the time point at which the normalized inversion recovery trace decays to 1/e of its initial value (see the Materials and Methods section). Figure 2 shows the plots of $\log(1/T_m)$ and $\log(1/T_1)$ vs the inverse of temperature for the spin label in perdeuterated glycerol (Figure 2A,B) and in DOTP (Figure 2C). The nitroxide reporter group in glycerol shows a distinct change in the temperature dependence of the transverse relaxation rate slightly above 190 K (Figure 2A); similarly, the temperature dependence of the longitudinal relaxation rate shows a smoother change at the same temperature (Figure 2B), corroborating the results obtained with the power saturation cw EPR technique (see Figure 1). The nitroxide reporter group in DOTP (Figure 2C) shows a sharper transition at 243 K in the temperature dependence of both relaxation rates, in analogy to the $\ln(P_{1/2})$ dependence presented in Figure 1.

Second, we considered a more complicated ternary mixture, containing as nitroxide reporter either SL1 in solution or an MTSL nitroxide spin label covalently attached to two water-soluble proteins in a glycerol/water solution (Figure 3). We selected two singly spin-labeled water-soluble proteins (T4-lysozyme and the maltose binding protein MalE) labeled at solvent-exposed sites. The T_g of a 50% v/v water/glycerol mixture (~0.2 molar fraction) is 175 K.[32] Notably, for pure water, there is a debate concerning the T_g at ambient pressure and the magnitude of the associated discontinuity of the specific heat. Extrapolation of T_g in binary aqueous solutions, in the limit of vanishing solute concentration, provides the estimated T_g of ~136 K ($1/T = 0.0073$),[33] but this conventionally accepted value has been challenged (see, for example, refs 34 and 35).

The power saturation cw EPR analysis in Figure 3 showed remarkable differences compared to the binary systems (Figure 1). The plot of $\ln(P_{1/2})$ vs $1/T$ for the ternary system with SL1 glycerol and water (Figure 3A) shows a first change in the saturation at $T < 175$ K (T_g of the bulk solution with 50% v/v glycerol). Additionally, a discontinuity in the trend of $\ln(P_{1/2})$ vs $1/T$ is observed between 175 and 190 K, before a linear trend is again established at higher temperatures. Figure 3B shows the plot of $\ln(P_{1/2})$ vs $1/T$ for T4-lysozyme in buffer containing 30% (gray dots) and 50% v/v (black dots) glycerol-D_8, and Figure 3C shows the same plot obtained with spin-labeled MalE in buffer containing 50% v/v glycerol-D_8. The nitroxide reporter group at position 96 in T4-lysozyme shows a smooth change in the $\ln(P_{1/2})$ vs $1/T$ trend around 190 K (T_g of pure glycerol) for both glycerol contents, without detectable discontinuity in the 175−190 K temperature range. In contrast, the reporter nitroxide group at position 36 in MalE shows a first change in the slope of $\ln(P_{1/2})$ vs $1/T$ close to 175 K (T_g of 50% glycerol/water solution), and a detectable discontinuity between 175 and 190 K. This discontinuity occurs always close to the T_g of the bulk solvent but is present to different extents in the three tested systems. Such site-specificity suggests that the discontinuity and its molecular origin are modulated by the local environment of the nitroxide radical.

Next, we addressed the dependence of the discontinuity in the 175−190 K temperature region with respect to the thermal history of the sample by detecting separately the relaxation rates T_1 and T_m via pulsed EPR methods (Figure 4) on the ternary system SL1 in water/glycerol mixtures either shock-frozen in liquid nitrogen (condition defined as "before annealing") or after annealing of the sample at $T > 190$ K. Notably, −80 °C freezers lead to sample annealing. Figure 4 shows the trend of the relaxation rates before and after annealing. In the range 180−200 K, a discontinuity in both T_m and T_1 was detected only in the sample measured before annealing (Figure 4A), which

DOI: 10.1021/acs.jpcb.5b04104
J. Phys. Chem. B 2015, 119, 13797−13806

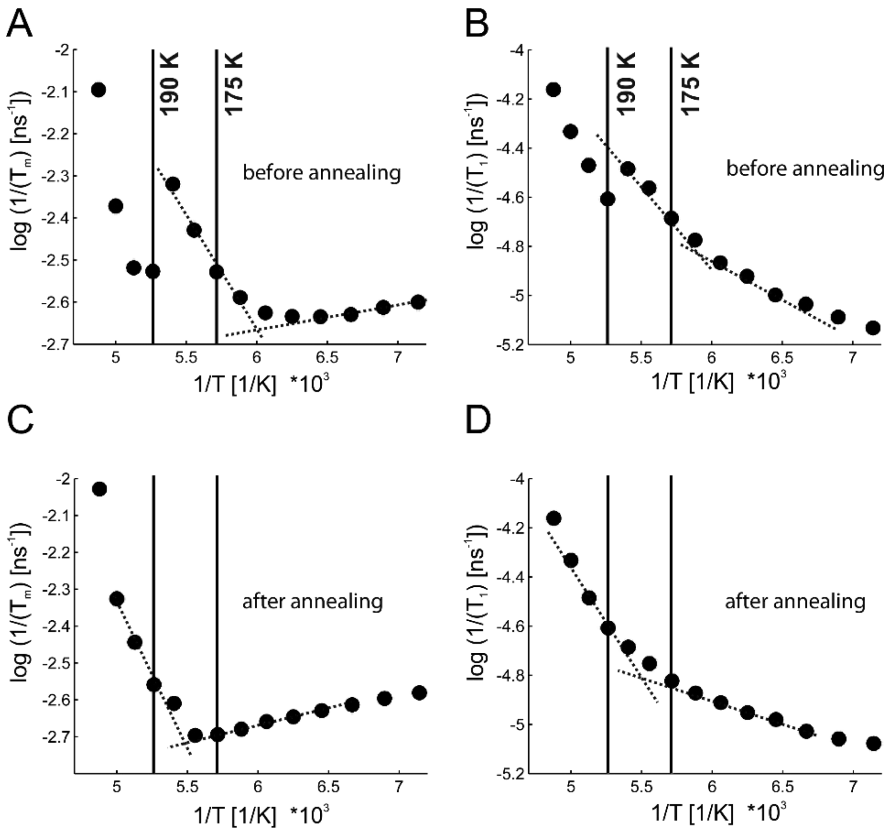

Figure 4. Effects of thermal history on the temperature dependence of relaxation rates of the reporter group SL1 in aqueous buffer with glycerol-D_8. (A) Plot of $\log(1/T_m)$ and (B) $\log(1/T_1)$ vs $1/T$ before annealing. The vertical lines represent the 175 K (T_g used in MMM for water/glycerol mixture) and 190 K (T_g of pure glycerol). The dotted lines guide the eye to highlight the first visible change in slope close to 165 K. The discontinuity between 175 and 190 K fully reproduces that observed with the power saturation method. (C) Plot of $\log(1/T_m)$ and (D) $\log(1/T_1)$ vs $1/T$ after annealing of the sample at $T > 190$ K. The vertical lines represent the 175 and 190 K temperatures as in panels A and B. The dotted lines guide the eye to highlight the visible change in slope close to 180 K.

corroborates the results obtained with power saturation cw methods (see Figure 3A). In contrast, after annealing, the discontinuity was absent, indicating that the thermal history of the sample modifies the local environment of the nitroxide group, and hence its relaxation rates in this particular temperature region (Figure 4C and D). After annealing, the trend of relaxation rates showed a unique change at about 180 K, similar to the single transition observed in the binary systems (Figure 2). Interestingly, the relaxation rates are slower in the 175−190 K temperature range with respect to the sample shock-frozen in liquid nitrogen; however, they do not show appreciable changes outside this "metastable" region.

To address the molecular origin of the discontinuity seen for shock-frozen samples in the 175−190 K temperature range both by power saturation cw EPR and by relaxation measurements, W-band cw EPR and EDNMR experiments were performed on SL2 dissolved in a 50% v/v D_2O/glycerol-D_8 mixture, where the discontinuity was detected, and in pure glycerol-D_8 where the discontinuity was absent.

These two methods allow the local nitroxide microenvironment to be characterized in terms of polarity and proticity, based on g_{xx} and A_{zz} magnetic parameters.[1−5]

The W-band cw EPR spectra for SL2 in solution of D_2O/glycerol-D_8 (50/50% v/v) recorded before and after annealing are presented in Figure 5A. In the g_{xx} spectral region, two nitroxide radical fractions with different g_{xx} values are present, and assigned to nitroxide radical populations forming different numbers of H-bonds with the solvent molecules.[3,4] The strong overlap of their EPR lines, however, limits the accuracy of the determination of the corresponding g^i_{xx} values. The spectra recorded before and after annealing can be simulated with the same set of magnetic parameters (the g^i_{xx} values used here are 2.00831 ± 0.00004 for a single H-bond (i = 1H) and 2.00790 ± 0.00004 for two H-bonds (i = 2H), as reported in ref 4). For the shock-frozen sample, the fraction of nitroxide radicals forming two H-bonds is predominant (about 60%), while after annealing it decreases to about 40%. Additionally, within experimental accuracy, the inhomogeneous EPR line width in the g_{zz} spectral region is not influenced by the annealing, but the average A_{zz} value changes by $\Delta A_{zz} = -2.5$ MHz. This shift can be rationalized in terms of a change in the ratio of nitroxide radical fractions characterized by different A_{zz} values.

To resolve the changes in the A_{zz} hyperfine coupling constants, describing two nitroxide radical fractions, we used W-band EDNMR[5] (Figure 5B). In contrast to power saturation techniques, this pulsed EPR technique works best for a spin system with sufficiently long T_m relaxation time; otherwise, high spin concentrations (>250 μM) are required for sufficient signal-to-noise ratio.[5] Figure 5B shows representative EDNMR data at the spectral position close to g_{zz}, $m_I = -1$, recorded before and after annealing (see also Figure S4). Two partially resolved pairs of lines centered at two different A_{zz} values are visible (green and blue lines in Figure 5B). To extract the A_{zz} values, EDNMR data at each magnetic field position were fitted to four Gaussian lines

DOI: 10.1021/acs.jpcb.5b04104
J. Phys. Chem. B 2015, 119, 13797−13806

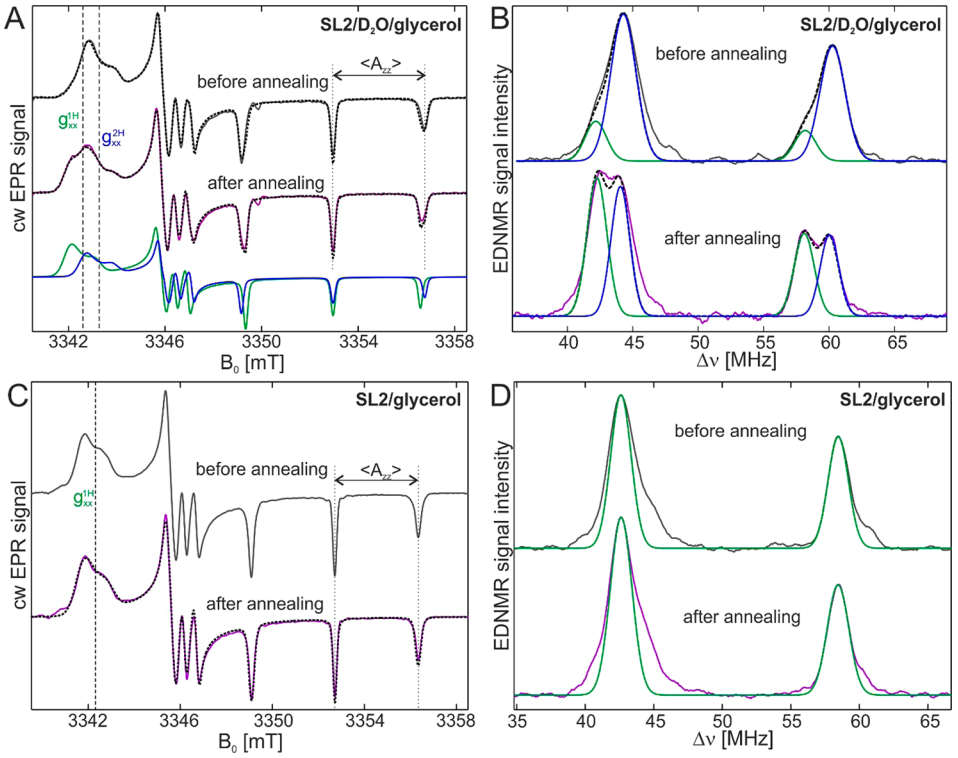

Figure 5. W-band cw EPR and EDNMR analysis of SL2 dissolved in 50% v/v water/glycerol mixture or in pure glycerol-D_8. (A) Experimental W-band cw EPR spectra of 1 mM SL2 in frozen solution of D_2O/glycerol-D_8 (50/50% v/v) recorded at 80 K before (gray trace) and after (purple trace) annealing of the sample for 1 h at 200 K. The spectral positions that correspond to different principal g_{xx} components (for one and two H-bonds to the nitroxide) and average A_{zz} values are indicated by dashed and dotted lines, respectively. The black dashed lines give the resulting simulated cw EPR spectra. The simulated spectral contributions corresponding to single (green trace) and double (blue trace) hydrogen bonded fractions after annealing are shown. (B) Experimental W-band EDNMR spectra of 1 mM SL2 in frozen solution of D_2O/glycerol-D_8 (50/50% v/v) taken under identical experimental settings at 80 K before (gray trace) and after (purple trace) annealing. The spectral contributions corresponding to single and double hydrogen bonded fractions of nitroxides are shown in green and blue, respectively. The black dashed lines give the resulting simulated EDNMR spectra. (C) Experimental W-band cw EPR spectra of 1 mM SL2 in frozen solution of glycerol-D_8 recorded at 80 K before (gray trace) and after (purple trace) annealing of the sample for 1 h at 230 K. The spectral positions that correspond to principal g_{xx} and A_{zz} components are indicated by dashed and dotted lines, respectively. The black dashed line gives the resulting simulated cw EPR spectrum using a single set of magnetic parameters. (D) Experimental W-band EDNMR spectra of 1 mM SL2 in frozen solution of glycerol-D_8 taken under identical experimental settings at 80 K before (gray trace) and after (purple trace) annealing the sample for 1 h at 230 K. The simulated spectral contribution corresponding to single hydrogen bonded nitroxide (green trace) is shown.

Table 1. A_{zz} Values and Fractions of Nitroxide Populations for SL2 in Frozen Solution of D_2O/Glycerol-D_8 or Glycerol-D_8 as Obtained from the Analysis of W-Band EDNMR at 80 K

	annealing	A^{1H}_{zz} (MHz)	fr^{1H}	A^{2H}_{zz} (MHz)	fr^{2H}
SL2 in 50% glycerol-D_8	before	101.6 ± 0.2	0.22 ± 0.04	106.1 ± 0.2	0.78 ± 0.04
	after	101.3 ± 0.2	0.47 ± 0.03	106.0 ± 0.2	0.53 ± 0.03
SL2 in 100% glycerol-D_8	before	101.9 ± 0.1	~0.80 ± 0.05[a]		
	after	101.8 ± 0.1	~0.80 ± 0.05[a]		

[a]On the basis of additional 244 GHz cw EPR measurements.

as described previously.[5] Figure 5B shows the example of the best fit to the experimental EDNMR recording for SL2 in frozen solution of D_2O/glycerol-D_8. After annealing, the weights of the two spectral components change in favor of a pair of lines centered around a smaller A_{zz} principal value (green line in Figure 5B), in agreement with the increased fraction of nitroxide radicals forming a single H-bond detected via low-temperature cw W-band in Figure 5A (see also Table 1 and Figure S5). The EDNMR line widths of about 2.3 ± 0.2 MHz directly report on the larger heterogeneity of the nitroxide local environment, reflected in the distribution of A_{zz} values, with respect to previously reported data in 2-propanol (line width of 1.2 ± 0.05 MHz).[5]

In contrast to the D_2O/glycerol-D_8 mixture, no changes in the g_{xx} spectral region of the W-band cw EPR spectrum could be observed after annealing when pure glycerol-D_8 was used as a solvent (Figure 5C and Figure S5), and the W-band cw EPR spectrum can be satisfactorily described with only a single set of magnetic parameters. Similarly, no changes in the W-band EDNMR recordings were observed before and after annealing, with one, dominating nitroxide fraction being the unique contribution to the spectra (Figure 5D and Table 1). This analysis proves that the discontinuity around the glass transition temperature detected by power saturation cw EPR and relaxation rates (Figures 3 and 4) on nitroxide probes in the presence of water is due to H-bond rearrangements toward the probe.

DOI: 10.1021/acs.jpcb.5b04104
J. Phys. Chem. B 2015, 119, 13797−13806

W-band EDNMR spectra were also recorded for one spin-labeled protein sample, namely T4-lysozyme, for which the discontinuity was absent in the power saturation data (Figure 3B); hence, no microenvironment changes are expected upon annealing. Indeed, only minor changes in the fractions of nitroxide populations were detected (Figure S7), reinforcing the explanation of the origin of the discontinuity. However, the reliable characterization of variations of local environment in spin-labeled proteins (with intrinsically broad EDNMR lines) requires a high spin concentration (>ca. 250 μM), which limits the application of this method in particular for membrane proteins.

To further address if the effects are solely due to local H-bonds to water molecules, we investigated the annealing effects under different glycerol contents (see Figure S6). Very similar effects were detected at W band for SL2 dissolved in D_2O with either 5, 10, or 50% glycerol-D_8 (v/v) (see Figure S6 and Table S1). It can be therefore concluded that the discontinuity observed in the power saturation experiments is exclusively due to reorganization of the H-bond network between the nitroxide radical and the water molecules.

DISCUSSION

This study shows that power saturation cw EPR using nitroxide radicals as reporter groups can be applied to extract local glass transition temperatures for simple binary systems without water (nitroxide/glycerol; nitroxide/*ortho*-terphenyl), as previously shown for spin-labeled polymers.[20−22] Interestingly, a smooth transition of the saturation properties of the reporter groups was detected for the nitroxide probe in pure glycerol, while a sharper transition was found for the more fragile glass former *ortho*-terphenyl. When the method is applied to ternary mixtures containing water (nitroxide/water/glycerol), a discontinuity in the power saturation behavior around the expected T_g was observed. Using high-field EPR methods, we found that this discontinuity originates from changes in the H-bond network toward the nitroxide probe around T_g. Shock freezing of the nitroxide/water/glycerol mixture from room temperature traps a large fraction of nitroxides with two H-bonds. Annealing above 180 K, which happens on its own when storing the sample in a conventional −80 °C freezer, decreases the 2H-bond fraction in favor of the 1H-bond fraction. After annealing, the discontinuity is absent, the "relaxed" T_1 and T_m values in the 170−190 K region can be measured, and reproducible fractions of the H-bonded nitroxide populations can be obtained using high-field EPR techniques.

It was early recognized that the rate of heating and cooling affects the determination of T_g (see, for example, ref 36). This is the reason why, in our experiments, after shock freezing of the sample, we kept a constant heating rate throughout the data acquisition. Clearly, longer equilibration (>30 min) at each temperature before detecting the power saturation data could have affected the extent of the discontinuity. In fact, after reaching 180 K, the relaxation rates determined by subsequent 2P-ESEEM experiments were progressively slowing down over a period of 20−30 min (data not shown), which indicates that providing more time for the system to equilibrate at temperatures close to T_g would have allowed the water molecules to rearrange toward the most energetically stable state, thereby decreasing the detectable discontinuity.

The preliminary experiments performed on two spin-labeled protein sites indicate that the power saturation technique is sufficiently sensitive to detect site-specific differences in the local environment around the glass transition temperature. In fact, the two protein samples showed either no discontinuity (T4-lysozyme) or a minor discontinuity (MalE), possibly due to distinct interactions between water molecules and the nitroxide radicals modulated by neighboring residues with different steric hindrances and/or charge distributions. Notably, these differences might also be due to enhanced local glycerol concentration around water-exposed sites in proteins compared to radicals in water/glycerol solution, which decreases the maximum fraction of nitroxides forming 2H-bonds in favor of the more stable 1H-bond situation, thereby reducing the discontinuity between 175 and 190 K in the $\ln(P_{1/2})$ vs $1/T$ plots.

When the energetically optimal H-bonding situation is achieved after annealing, observation of the glass transition via the saturation behavior is facilitated and the possible site-specific differences of local T_g values at different spin-labeled sites can be investigated. Interestingly, in the case of T4-lysozyme, which does not show the discontinuity, the EPR saturation parameters of the spin-labeled side chain at position 96 indicate a smooth transition around 190 K (Figure 3B). Such a smooth transition of the relaxation properties around T_g points to a microenvironment characterized by low fragility,[35] and it is consistent with the broad range of T_g values (160−190 K) found in hydrated protein systems (for recent reviews, see refs 37 and 38). In particular, for hydrated lysozyme, an approximate $T_g \sim 180 \pm 15$ K was reported (see, for example, ref 39), which originates from the collective motion due to the so-called main structural relaxation (α-relaxation) in hydrated proteins (for two recent reviews, see refs 40 and 41).

In conclusion, we show that the relaxation parameters of nitroxide radicals are extremely sensitive to changes in the coordination of the nitroxides by H-bonded water molecules. Such changes occur close to the glass transition temperature of their microenvironment, providing a new interesting tool to monitor subtle molecular effects in this temperature range. Note that the change in the H-bonding to neighboring water molecules around T_g is an inherent property of the chosen type of nitroxide label, and may thus not provide direct information on the microenvironment of native side chains in proteins. Additional biophysical experiments performed on native protein samples with a controlled thermal history could clarify this point. This newly discovered H-bonding rearrangement of the microenvironment of nitroxide probes around T_g also has important implications for the low-temperature high-field EPR studies of the nitroxide-labeled systems. For example, to obtain reliable polarity/proticity information on nitroxides in frozen protein samples, it is necessary to either (i) choose a reproducible annealing methodology or (ii) analyze all samples immediately after shock freezing or (iii) store them constantly in liquid nitrogen, well below the glass transition temperature of the water/glycerol mixture. Among these procedures, (i) is expected to lead to the best reproducibility, since thermal history is hard to control during shock freezing. An annealing protocol is thus also recommended for studies that do not explicitly address the microenvironment but might be affected by variation in relaxation times. However, in order to obtain information related to site-specific water coordination at ambient temperature, annealing must be avoided.

ASSOCIATED CONTENT

Supporting Information

The Supporting Information is available free of charge on the ACS Publications website at DOI: 10.1021/acs.jpcb.5b04104.

DOI: 10.1021/acs.jpcb.5b04104
J. Phys. Chem. B 2015, 119, 13797−13806

Figures showing cw EPR spectra and power saturation curves, plot of $\ln(P_{1/2})$ vs $1/T$, echo-detected field sweep and relaxation measurements, W-band EDNMR recordings, high-field cw EPR and EDNMR analysis, and experimental W-band EDNMR spectra and table with magnetic parameters (PDF)

AUTHOR INFORMATION

Corresponding Author

*E-mail: enrica.bordignon@fu-berlin.de. Phone: +49(0)30 838 54629.

Author Contributions

The manuscript was written through contributions of all authors. All authors have given approval to the final version of the manuscript.

Notes

The authors declare no competing financial interest.

ACKNOWLEDGMENTS

This work is supported by the Cluster of Excellence RESOLV (EXC 1069) funded by the Deutsche Forschungsgemeinschaft and the Max-Planck-Gesellschaft (A.S.). E.B. and A.S. would like to thank Herbert Zimmermann (Max Planck Institute for Medical Research, Heidelberg) for having provided the SL2 nitroxide spin radical, the deuterated form of the SL1 nitroxide spin radical, and *ortho*-terphenyl-D_{14},; E.B. would like to thank B. Joseph for preparing the T4-lysozyme sample and E. Schneider for the MalE sample.

ABBREVIATIONS

EDNMR, ELDOR-detected NMR; T_g, glass transition temperature; cw, continuous wave

REFERENCES

(1) Plato, M.; Steinhoff, H.-J.; Wegener, C.; Törring, J. T.; Savitsky, A.; Möbius, K. Molecular orbital study of polarity and hydrogen bonding effects on the g and hyperfine tensors of site directed NO spin labelled bacteriorhodopsin. *Mol. Phys.* **2002**, *100* (23), 3711−3721.

(2) Steinhoff, H.-J.; Savitsky, A.; Wegener, C.; Pfeiffer, M.; Plato, M.; Möbius, K. High-field EPR studies of the structure and conformational changes of site-directed spin labeled bacteriorhodopsin. *Biochim. Biophys. Acta, Bioenerg.* **2000**, *1457* (3), 253−262.

(3) Bordignon, E.; Brutlach, H.; Urban, L.; Hideg, K.; Savitsky, A.; Schnegg, A.; Gast, P.; Engelhard, M.; Groenen, E. J. J.; Möbius, K.; Steinhoff, H.-J. Heterogeneity in the Nitroxide Micro-Environment: Polarity and Proticity Effects in Spin-Labeled Proteins Studied by Multi-Frequency EPR. *Appl. Magn. Reson.* **2010**, *37* (1−4), 391−403.

(4) Gast, P.; Herbonnet, R. T. L.; Klare, J.; Nalepa, A.; Rickert, C.; Stellinga, D.; Urban, L.; Mobius, K.; Savitsky, A.; Steinhoff, H.-J.; Groenen, E. J. J. Hydrogen bonding of nitroxide spin labels in membrane proteins. *Phys. Chem. Chem. Phys.* **2014**, *16* (30), 15910−15916.

(5) Nalepa, A.; Möbius, K.; Lubitz, W.; Savitsky, A. High-field ELDOR-detected NMR study of a nitroxide radical in disordered solids: Towards characterization of heterogeneity of microenvironments in spin-labeled systems. *J. Magn. Reson.* **2014**, *242* (0), 203−213.

(6) Carmieli, R.; Papo, N.; Zimmermann, H.; Potapov, A.; Shai, Y.; Goldfarb, D. Utilizing ESEEM spectroscopy to locate the position of specific regions of membrane-active peptides within model membranes. *Biophys. J.* **2006**, *90* (2), 492−505.

(7) Volkov, A.; Dockter, C.; Bund, T.; Paulsen, H.; Jeschke, G. Pulsed EPR determination of water accessibility to spin-labeled amino acid residues in LHCIIb. *Biophys. J.* **2009**, *96* (3), 1124−41.

(8) Altenbach, C.; Froncisz, W.; Hubbell, W. L. Quantitative determination of collision frequency between spin labels and dissolved paramagnetic reagents. *Biophys. J.* **2002**, *82* (1), 479a−480a.

(9) Altenbach, C.; Greenhalgh, D. A.; Khorana, H. G.; Hubbell, W. L. Epr Depth Measurements of Nitroxides in Membrane Bilayers Using Spin Labeled Mutants of Bacteriorhodopsin. *Biophys. J.* **1993**, *64* (2), A51−A51.

(10) Altenbach, C.; Greenhalgh, D. A.; Khorana, H. G.; Hubbell, W. L. A collision gradient-method to determine the immersion depth of nitroxides in lipid bilayers - Application to spin-labeled mutants of bacteriorhodopsin. *Proc. Natl. Acad. Sci. U. S. A.* **1994**, *91* (5), 1667−1671.

(11) Perozo, E.; Cortes, D. M.; Cuello, L. G. Three-dimensional architecture and gating mechanism of a K+ channel studied by EPR spectroscopy. *Nat. Struct. Biol.* **1998**, *5* (6), 459−469.

(12) Pyka, J.; Ilnicki, J.; Altenbach, C.; Hubbell, W. L.; Froncisz, W. Accessibility and dynamics of nitroxide side chains in T4 lysozyme measured by saturation recovery EPR. *Biophys. J.* **2005**, *89* (3), 2059−2068.

(13) Doll, A.; Bordignon, E.; Joseph, B.; Tschaggelar, R.; Jeschke, G. Liquid State DNP for Water Accessibility Measurements on Spin-labeled Membrane Proteins at Physiological Temperatures. *J. Magn. Reson.* **2012**, *222*, 34−43.

(14) Cheng, C.-Y.; Han, S. Dynamic Nuclear Polarization Methods in Solids and Solutions to Explore Membrane Proteins and Membrane Systems. *Annu. Rev. Phys. Chem.* **2013**, *64* (1), 507−532.

(15) Eaton, G. R.; Eaton, S. S.; Weber, R. T. Temperature. In *Quantitative EPR*; Eaton, G. R., Eaton, S. S., Barr, D. P., Weber, R. T., Eds.; Springer-Verlag: Wien, Austria, 2010; pp 91−99.

(16) Georgieva, E. R.; Roy, A. S.; Grigoryants, V. M.; Borbat, P. P.; Earle, K. A.; Scholes, C. P.; Freed, J. H. Effect of freezing conditions on distances and their distributions derived from Double Electron Electron Resonance (DEER): A study of doubly-spin-labeled T4 lysozyme. *J. Magn. Reson.* **2012**, *216* (0), 69−77.

(17) Polyhach, Y.; Bordignon, E.; Jeschke, G. Rotamer libraries of spin labelled cysteines for protein studies. *Phys. Chem. Chem. Phys.* **2011**, *13* (6), 2356−2366.

(18) Hagelueken, G.; Ward, R.; Naismith, J. H.; Schiemann, O. MtsslWizard: In Silico Spin-Labeling and Generation of Distance Distributions in PyMOL. *Appl. Magn. Reson.* **2012**, *42* (3), 377−391.

(19) Jeschke, G. Conformational dynamics and distribution of nitroxide spin labels. *Prog. Nucl. Magn. Reson. Spectrosc.* **2013**, *72*, 42−60.

(20) Miwa, Y. Novel and Accurate Method for Determination of Glass Transition Temperature of Spin-Labeled Polymer by ESR Microwave Power Saturation. *Macromolecules* **2009**, *42* (16), 6141−6146.

(21) Miwa, Y.; Yamamoto, K. Simple and Highly Sensitive Measurement Method for Detection of Glass Transition Temperatures of Polymers: Application of ESR Power Saturation Phenomenon with Conventional Spin-Probe Technique. *J. Phys. Chem. B* **2012**, *116* (30), 9277−9284.

(22) Miwa, Y.; Urakawa, O.; Doi, A.; Yamamoto, K.; Nobukawa, S. Glass Transition Temperature and β Relaxation Temperature around Chain End of Polystyrene Determined by Site Specific Spin Labeling. *J. Phys. Chem. B* **2012**, *116* (4), 1282−1288.

(23) Mchaourab, H.; Fang, C. S.; Hubbell, W. L. A site-directed spin labeling study of T4 lysozyme solution structure. *Biophys. J.* **1996**, *70* (2), Mp120−Mp120.

(24) Columbus, L.; Kalai, T.; Jeko, J.; Hideg, K.; Hubbell, W. L. Mapping backbone dynamics with site-directed spin labeling. *Biophys. J.* **2001**, *80* (1), 174a−174a.

(25) Bohm, S.; Licht, A.; Wuttge, S.; Schneider, E.; Bordignon, E. Conformational plasticity of the type I maltose ABC importer. *Proc. Natl. Acad. Sci. U. S. A.* **2013**, *110* (14), 5492−5497.

(26) Portis, A. M. Rapid Passage Effects in Electron Spin Resonance. *Phys. Rev.* **1955**, *100* (4), 1219−1221.

(27) Weger, M. Passage Effects in Paramagnetic Resonance Experiments. *Bell Syst. Tech. J.* **1960**, *39* (4), 1013−1112.

(28) Savitsky, A.; Dubinskii, A. A.; Plato, M.; Grishin, Y. A.; Zimmermann, H.; Möbius, K. High-Field EPR and ESEEM

DOI: 10.1021/acs.jpcb.5b04104
J. Phys. Chem. B 2015, 119, 13797−13806

Investigation of the Nitrogen Quadrupole Interaction of Nitroxide Spin Labels in Disordered Solids: Toward Differentiation between Polarity and Proticity Matrix Effects on Protein Function. *J. Phys. Chem. B* **2008**, *112* (30), 9079−9090.
(29) Ryabov, Y. E.; Hayashi, Y.; Gutina, A.; Feldman, Y. Features of supercooled glycerol dynamics. *Phys. Rev. B: Condens. Matter Mater. Phys.* **2003**, *67* (13), 132202.
(30) Richert, R. On the dielectric susceptibility spectra of supercooled o-terphenyl. *J. Chem. Phys.* **2005**, *123* (15), 154502.
(31) Petzold, N.; Rössler, E. A. Light scattering study on the glass former o-terphenyl. *J. Chem. Phys.* **2010**, *133* (12), 124512.
(32) Hayashi, Y.; Puzenko, A.; Balin, I.; Ryabov, Y. E.; Feldman, Y. Relaxation Dynamics in Glycerol−Water Mixtures. 2. Mesoscopic Feature in Water Rich Mixtures. *J. Phys. Chem. B* **2005**, *109* (18), 9174−9177.
(33) Ghormley, J. A. Warming Curves for the Condensed Product of Dissociated Water Vapor and for Hydrogen Peroxide Glass. *J. Am. Chem. Soc.* **1957**, *79* (8), 1862−1865.
(34) Giovambattista, N.; Angell, C. A.; Sciortino, F.; Stanley, H. E. Glass-Transition Temperature of Water: A Simulation Study. *Phys. Rev. Lett.* **2004**, *93* (4), 047801.
(35) Angell, C. A. Liquid Fragility and the Glass Transition in Water and Aqueous Solutions. *Chem. Rev. (Washington, DC, U. S.)* **2002**, *102* (8), 2627−2650.
(36) Moynihan, C. T.; Easteal, A. J.; Wilder, J.; Tucker, J. Dependence of the glass transition temperature on heating and cooling rate. *J. Phys. Chem.* **1974**, *78* (26), 2673−2677.
(37) Doster, W. The protein-solvent glass transition. *Biochim. Biophys. Acta, Proteins Proteomics* **2010**, *1804* (1), 3−14.
(38) Roos, Y. H.; Potes, N. Quantification of Protein Hydration, Glass Transitions, and Structural Relaxations of Aqueous Protein and Carbohydrate−Protein Systems. *J. Phys. Chem. B* **2015**, *119* (23), 7077−7086.
(39) Khodadadi, S.; Malkovskiy, A.; Kisliuk, A.; Sokolov, A. P. A broad glass transition in hydrated proteins. *Biochim. Biophys. Acta, Proteins Proteomics* **2010**, *1804* (1), 15−19.
(40) Khodadadi, S.; Sokolov, A. P. Protein dynamics: from rattling in a cage to structural relaxation. *Soft Matter* **2015**, *11* (25), 4984−4998.
(41) Lewandowski, J. R.; Halse, M. E.; Blackledge, M.; Emsley, L. Direct observation of hierarchical protein dynamics. *Science* **2015**, *348* (6234), 578−581.

DOI: 10.1021/acs.jpcb.5b04104
J. Phys. Chem. B 2015, 119, 13797−13806